Comparative extreme ultraviolet emission measurements for lithium and tin laser plasmas

Simi A. George, William T. Silfvast, Kazutoshi Takenoshita, Robert T. Bernath, Chiew-Seng Koay, Gregory Shimkaveg, and Martin C. Richardson

Laser Plasma Laboratory, College of Optics and Photonics: CREOL and FPCE, University of Central Florida, Orlando, Florida 32816, USA

Received January 3, 2007; revised January 22, 2007; accepted January 23, 2007;
posted January 25, 2007 (Doc. ID 78682); published March 19, 2007

Detailed spectroscopic studies on extreme UV emission from laser plasmas using tin and lithium planar solid targets were completed. At 13.5 nm, the best conversion efficiency (CE) for lithium was found to be 2.2% at intensities near 7×10^{10} W/cm^2. The highest CE measured for tin was near 5.0% at an intensity close to 1×10^{11} W/cm^2. © 2007 Optical Society of America

OCIS codes: 300.6540, 340.7470, 020.0020.

To keep pace with Moore's law in the advancement of microprocessor technology while decreasing the cost per function, innovative lithographic techniques are required. Extreme ultraviolet (EUV) lithography[1] is identified as the next-generation lithography for printing integrated circuits with feature sizes below 32 nm. Since EUV radiation is absorbed in the atmosphere, a vacuum environment is required, and instead of transmissive optics, special reflective optics as well as reflective masks are needed at the optimum wavelength of 13.5 nm.[1,2] A light source that meets industry requirements[3] is one of the major challenges facing the cost-effective implementation of an EUV stepper tool. A suitable EUV light source must be efficient, spectrally clean, with minimal or no debris emanation for preservation of the expensive multilayer mirrors[3] (MLMs). EUV can be generated in a number of ways, but the most economical methods under consideration for lithography are pulsed-source architectures, laser-produced plasmas, and gas-discharge-produced plasmas.[4]

Laser plasmas are compact, intense light sources and are advantageous because of their power scalability, high repetition rates and thus greater dose stability, small source size with large solid angle for collection, and energy stability. Few materials are efficient emitters of 13.5 nm radiation. At present, three sources are being considered for EUV lasers (EUVLs); they are xenon,[5,6] tin,[6] and lithium.[7–9] Of these, tin and lithium targets are the two most likely to produce the output power levels required for high volume manufacturing.

A focused pulsed laser beam irradiating a target surface creates a rapidly expanding plasma with temperatures and densities sufficient to produce emission in the EUV. Emission characteristics are directly dependent on the plasma temperature and density distribution and are influenced by laser parameters, target composition, and geometry. Laser beam intensity, which is a function of beam focal area, beam energy, and pulse duration, is a key factor in obtaining optimum temperature and densities for 13.5 nm emission. In this Letter a direct comparison of EUV emission from tin and lithium planar solid targets for a variety of experimental parameters is presented. Through detailed spectroscopic studies, optimum EUV emission and efficiency were measured and compared for both targets.

Efficiency of the laser plasma light source or the conversion efficiency (CE) is defined as the ratio of usable EUV energy measured at 13.5 nm in the 2% reflectance bandwidth of the Mo/Si MLM mirror to laser energy input. The measured EUV energy radiated by the source across 2π sr solid angle (assuming isotropic emission) and within the 2% bandwidth (centered on 13.50 nm), is given by,[6,10,11]

$$E_{\mathrm{BW}} = \frac{2\pi A_{\mathrm{scope}}}{\Omega R_{\mathrm{scope}}\eta_{\mathrm{diode}}} \frac{\int_{\mathrm{BW}} I_{\mathrm{s}}(\lambda)\mathrm{d}\lambda}{\int_{\mathrm{all}} I_{\mathrm{s}}(\lambda)T_{\mathrm{g}}(\lambda)R_{\mathrm{mir}}(\lambda)T_{\mathrm{f}}(\lambda)\mathrm{d}\lambda}, \quad (1)$$

where A_{scope} is the integrated area under the EUV signal waveform displayed on an oscilloscope, R_{scope} is the oscilloscope impedance in ohms, $T_g(\lambda)$ is the correction for gas transmission conditions, $R_{\mathrm{mir}}(\lambda)$ is the calibrated mirror reflectivity, $T_f(\lambda)$ is the correction for transmission of filter(s) used to select EUV light, η_{diode} is the responsivity of the EUV diode detector in units of amperes per watt, $I_s(\lambda)$ is the measured spectral distribution of the EUV source in arbitrary units, and $\boldsymbol{\Omega}$ is the limiting solid angle from the source to detector. The solid angle $\boldsymbol{\Omega}$ is determined by $(\frac{1}{4}\pi D^2)/(L^2)$, where D is the diameter of the limiting aperture to the detector and L is the distance from the source to the limiting aperture.

The laser used for these studies is a commercially available Q-switched Nd:YAG system with maximum attainable energy of approximately 200 mJ per pulse at 1064 nm. The laser pulse duration (FWHM) is 10.5 ns with output beam diameter of 9 mm. A 50 mm diameter, antireflection coated, 100 mm focal length planoconvex lens was used to focus the beam onto the sample surface in p polarization at an angle of 45°. A detailed map of the focal region was obtained by imaging the beam focus with a 10× microscope objective on to a Spiricon SP980M CCD camera. Thus laser irradiation intensity at target for a given spectral measurement can be calculated. The minimum spot size achieved was 30 μm within error limits, and the lens was translated longitudinally to vary the spot size, changing the peak intensity. Background gas pressure below 4×10^{-6} Torr was maintained during experiments.

High-resolution spectra were obtained by using a flat-field grazing-incidence grating spectrograph,[12,13] which has a fixed entrance slit and a variably spaced concave grating with an average of 1200 lines/mm, providing a wavelength imaging range of 5–20 nm. Images of the EUV spectra were obtained by using a microchannel plate EUV detector in a chevron configuration, fiber optically coupled to a Photometrics 300 series, 1024×1024, 24 μm pixel, cooled spectroscopic CCD. During experiments the laser was operated at 2 Hz, and a shutter was used to generate single-shot spectra. The target surface was also translated parallel to itself to obtain a fresh surface for each measurement. Tin and lithium were both used in a single target mount to switch between metals without pause or vacuum venting. To measure the EUV energy, a diagnostic consisting of a 22 V biased AXUV-100G diode with an efficiency of 0.24 A/W was used in combination with a 45° Mo/Si MLM and a 0.5 μm zirconium filter. Reflectivity of the MLM and transmission of the zirconium filter was calibrated by the National Institute of Standards and Technology (NIST). The EUV diagnostic was placed inside the chamber and aligned normal to the target surface. The limiting aperture is the diameter of the zirconium filter diaphragm mount (7.1 mm) after the MLM, located 120 mm from the plasma source, resulting in a collecting solid angle of 2.75×10^{-3} sr. This EUV energy meter was calibrated against the Flying Circus[6,11] EUV diagnostic instrument with calibrated optics and a solid angle of 5.0×10^{-4} sr to ensure proper accounting of EUV energy. Descriptions of the EUV measurements, calibration methods, and method for calculating CE were presented in detail previously.[6]

Spectra were collected for a given input laser energy as a function of intensity, for both tin and lithium targets, to further optimize emission temperature of the plasma. Initial experimental results and theoretical comparisons were presented, previously.[14] Spectra as a function of intensity for lithium and tin solid targets are shown in Fig. 1. In the lithium spectra [Fig. 1(a)] the emission lines from the heliumlike $Li^{+}(1s-2p)$ transition at 19.9 nm and hydrogenlike transitions $Li^{2+}(1s-2p)$ at 13.5 nm, $Li^{2+}(1s-3p)$ at 11.39 nm, and $Li^{2+}(1s-4p)$ at 10.8 nm can be clearly identified. The most intense of these emission lines is the $Li^{2+}(1s-2p)$ at 13.5 nm, which is produced at plasma temperatures greater than 10 eV. The emission at 13.5 nm was found to be optimum for the intensity region of $1-5\times10^{11}$ W/cm^2. For lithium, the last resolvable transition before quasi-continuum is the $Li^{2+}(1s-5p)$ at 10.5 nm. Based on the Inglis–Teller limit,[15] an estimate of the upper bound on plasma electron density in the EUV emitting region is taken as 9.0×10^{19} cm^{-3}. The average plasma temperature calculated by using the ratios of observed line intensities of successive ionization stages, and the above electron density, is approximately 14 eV. This temperature estimation is valid if the transition levels are in local thermodynamic equilibrium with higher quantum levels, an assumption that is appropriate for the plasma region close to the target surface.[7,16]

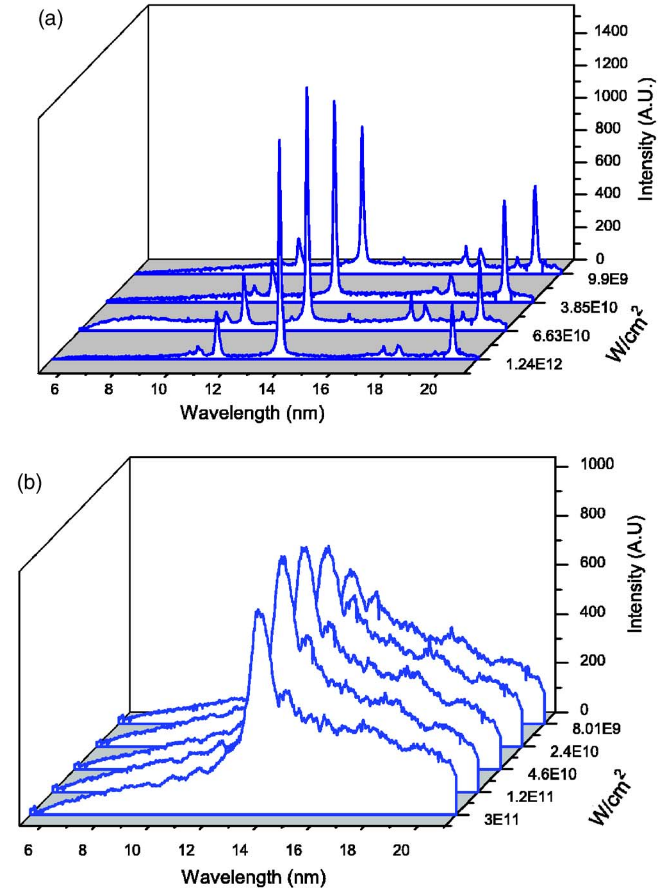

Fig. 1. (Color online) (a) Lithium spectral distribution for laser intensities ranging from 10^9-10^{11} W/cm^2; laser energy used is 65.5 mJ. (b) Tin spectra recorded for varying intensities with optimum emission at $1-2\times10^{11}$ W/cm^2 for the same experimental conditions as lithium.

Tin spectra [Fig. 1(b)] show the expected unresolved transition array (UTA) emission originating from the Sn^{7+} to Sn^{12+} ions with the ground configuration [Kr] $4p^6\ 4d^n$, where $n=2$ to 7.[6,17,18] The thousands of tin emission lines in the spectral region around 13.5 nm originate from transitions between the excited configurations, $4p^5 4d^{n+1}$ and $4p^6 4d^{n-1} 4f^1$.[17,19] Maximum emission at 13.5 nm is found to be at intensities in the region of $1-2\times10^{11}$ W/cm^2 with a plasma temperature of about 30 eV,[6,19] obtained from numerical simulations.

Both tin and lithium data sets (Fig. 1) show similar behavior, where the emission into 13.5 nm decreases with higher than optimum intensity. Previous research on tin-doped droplets has shown that tin emission into the 13.5 nm is strongest in the intensity region of $1-2\times10^{11}$ W/cm^2.[6] The spectral data also show that the lithium line emission is almost twice as intense in counts as the tin UTA at 13.5 nm.

Calibrated CE measurements using the EUV diagnostic were completed for each spectral measurement, thus providing a detailed map of the EUV emission with respect to intensity for both tin and lithium (Fig. 2). Results of the initial experiments were previously published, with 2.1% CE from lithium near 1.6×10^{11} W/cm^2, and 4.0% from tin near 1.2×10^{11} W/cm^2.[14] Transmission through the background gas was neglected, since EUV absorption is minimal at the background pressure conditions used. The maximum CE measured was 2.2% in lithium at an intensity of 6.6×10^{10} W/cm^2. For tin, the highest CE obtained is 4.9% at laser intensities near 9.2×10^{10} W/cm^2. Small scatter in the CE data is attributed to the target surface roughness on the sub-100 μm scale.

In summary, for EUVL to be successful, high-power sources with long lifetime are a requirement. We have optimized 13.5 nm emission for both tin and lithium. Single, intense line emission from lithium at 13.5 nm makes this source a strong candidate for lithography light source. UTA emission in tin is less intense as compared with lithium line emission, but the greater number of photons emitted within the useful bandwidth results in higher conversion efficiencies. The CE measurements for planar tin are comparable with previous findings from experiments completed by using a completely different collection regime.[6,18] Quantification of full spectral out-of-band emission from tin for optimal CE emission condition is still needed. Also needed are detailed debris analyses for determining source lifetime, as well as EUV angular distribution measurements for better accounting of CE.

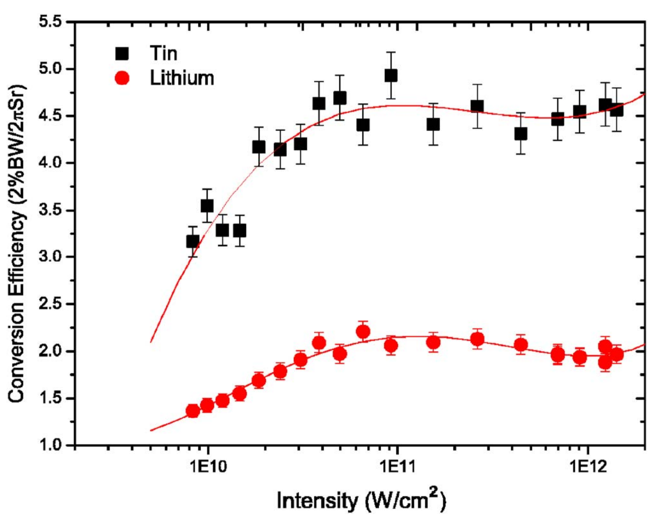

Fig. 2. (Color online) Conversion efficiency as function of intensity for lithium and tin into 2% bandwidth and 2π sr. Laser energy used for these measurements is 78.6 mJ. The highest CE obtained for tin is 4.9% at an irradiance intensity of 9×10^{11} W/cm^2, and for lithium the highest is 2.2% near 6.6×10^{10} W/cm^2.

The authors acknowledge technical support from Somsak Teerawattanasook and Jose Cunado. We greatly appreciate the reflectometry measurements for calibration provided by Steven Grantham of the Photon Physics Group at NIST. Funding for this project is provided by the State of Florida and Sematech. S. George's e-mail address is sgeorge@creol.ucf.edu; M. Richardson's, mcr@creol.ucf.edu.

References

1. C. W. Gwyn, R. Stulen, D. Sweeney, and D. Attwood, J. Vac. Sci. Technol. B **16**, 3142 (1998).
2. W. T. Silfvast, IEEE J. Quantum Electron. **35**, 700 (1999).
3. K. Ota, Y. Watanabe, H. Franken, and V. Banine, "EUV source requirements," presented at the EUV Source Workshop, Third International EUVL Symposium, Miyazaki, Japan, November 5, 2004.
4. M. A. Klosner, H. A. Bender, and W. T. Silfvast, Opt. Lett. **22**, 34 (1997).
5. M. A. Klosner and W. T. Silfvast, Opt. Lett. **23**, 1609 (1998).
6. C.-S. Koay, S. George, K. Takenoshita, R. Bernath, E. Fujiwara, M. C. Richardson, and V. Bakshi, Proc. SPIE **5751**, 279 (2005).
7. D. J. O'Connell, "Characterization of a lithium laser produced plasma at 135 Å for extreme ultraviolet projection lithography," M.S. thesis (University of Central Florida, 1994).
8. I. V. Fomenkov, W. N. Partlo, N. R. Böwering, A. I. Ershov, C L. Rettig, R. M. Ness, I. R. Oliver, S. T. Melnychuk, O. V. Khodykin, J. R. Hoffman, V. B. Fleurov, J. M. Algots, J. W. Viatella, B. A. M. Hansson, O. Hemberg, A. N. Bykanov, E. A. Lopez, P. C. Oh, T. D. Steiger, and D. W. Myers, "Progress in development of a high power source for EUV lithography," presented at the Symposium on EUVL (Miyasaki, Japan), November 1–5, 2004.
9. D. Myers, B. Klene, I. Fomenkov, B. Hansson, and B. Bolloger, "The optimal path to HVM," presented at the Symposium on EUVL (Miyasaki, Japan), November 1–5, 2004.
10. "FC2: Calibration of a EUV Source at PLEX LLC" (International SEMATECH Technology Transfer no. 04024490A-TR).
11. R. Stuik, F. Scholze, J. Tummler, and F. Bijkerk, Nucl. Instrum. Methods Phys. Res. A **429**, 305 (2002).
12. W. Schwanda, K. Eidmann, and M. C. Richardson, J. X-Ray Sci. Technol. **4**, 8 (1993).
13. T. Kita, T. Harada, N. Takano, and H. Kuroda, Appl. Opt. **22**, 512 (1983).
14. S. A. George, W. Silfvast, K. Takenoshita, R. Bernath, C.-S. Koay, G. Shimkaveg, M. Al-Rabban, H. Scott, and M. Richardson, Proc. SPIE 6151 (2006).
15. H. R. Griem, *Spectral Line Broadening by Plasmas* (New York, 1974).
16. H. R. Griem, *Plasma Spectroscopy* (McGraw-Hill, 1964).
17. W. Svendsen and G. O'Sullivan, Phys. Rev. A **50**, 3710 (1994).
18. S. George, C.-S. Koay, K. Takenoshita, R. Bernath, M. Al-Rabban, C. Keyser, H. Scott, V. Bakshi, and M. C. Richardson, Proc. SPIE **5751**, 779 (2005).
19. M. Al-Rabban, C. Keyser, S. George, H. Scott, V. Bakshi, and M. C. Richardson, Proc. SPIE **5751**, 769 (2005).